

# Elastic Polyaniline with EPDM and Dodecylbenzenesulfonic Acid as Plasticizers

ROSELENA FAEZ, MARCO-A DE PAOLI

Laboratório de Polímeros Condutores e Reciclagem, Instituto de Química, Universidade Estadual de Campinas, C. Postal 6154, 13083-970 Campinas-SP, Brasil

Received 25 October 2000; accepted 23 February 2001

**ABSTRACT:** Elastomeric polyaniline was prepared by being mixed with ethylene-propylene-diene (EPDM) rubber in low concentrations (10, 20, or 30 wt %). The mixture was made in an internal mixer coupled to a torque rheometer. The polyaniline was doped with dodecylbenzenesulfonic acid (DBSA) via reactive processing during the mixing. When the EPDM rubber was added to the polyaniline and DBSA, the doping reaction was not interrupted, as demonstrated by an increase in the torque values. We chose the relative DBSA and EPDM concentrations to obtain the highest conductivities ( $10^{-1}$  to  $10^{-3}$  S cm $^{-1}$ ) and the best mechanical properties. © 2001 John Wiley & Sons, Inc. *J Appl Polym Sci* 82: 1768–1775, 2001

**Key words:** polyaniline; processing; elastomers; mechanical properties; conducting polymer

## INTRODUCTION

Polyaniline (PAni) is a promising conducting polymer for practical applications because of its high thermal stability, easy preparation, and low-cost monomer. However, its inherent brittleness and lack of processability limit many commercial uses. Many efforts have been made to improve its mechanical properties and expand its applicability. Attempts to improve its mechanical properties have been mostly directed toward the preparation of film polymers by the ordinary casting method.<sup>1,2</sup> Significant progress in the preparation of processable forms of PAni was recently reported. Solution processing of the conductive form of PAni was attained with sulfonic acids,<sup>3,4</sup> phosphonic acids, and phosphoric acid diesters<sup>5–7</sup> as

protonating agents. In addition, some PAni dopants plasticize it upon protonation, which, in turn, facilitates thermal processing. Two specific functional acids, camphorsulfonic acid (CSA) and dodecylbenzenesulfonic acid (DBSA), have been used in various organic solvents such as *m*-cresol and *n*-methylpyrrolidone (NMP).<sup>8</sup> Despite the possibility of solution processing, solvent evaporation may cause environmental problems, and any residual solvent might modify the material properties.

Ethylene-propylene-diene (EPDM) rubber has been used extensively as an impact modifier for polyolefins,<sup>9</sup> remarkably improving their mechanical properties. The rubber has two functions: it relieves the volume strain by cavitation, and it acts as a stress concentrator. Both functions depend on the rubber concentration.<sup>10</sup>

In this study, PAni doping was achieved by the introduction of the dopant molecule into the solid undoped polymer without the use of an auxiliary solvent. Complex formation in the solid phase occurred at an elevated temperature and resulted in the formation of a soluble and processable con-

Correspondence to: M.-A. De Paoli (mdepaoli@iqm.unicamp.br).

Contract grant sponsor: Fundação de Amparo à Pesquisa do Estado de São Paulo; contract grant numbers: 95/01457-4 and 96/09983-6.

*Journal of Applied Polymer Science*, Vol. 82, 1768–1775 (2001)  
© 2001 John Wiley & Sons, Inc.

ducting complex.<sup>11,12</sup> Here, *processability* is understood as the condition of being processable by methods currently used by the industry for large-scale production. To improve mechanical properties, we also used EPDM during the doping stage, eliminating the auxiliary solvent. The aim of this study was to show how EPDM could be used as a mechanical-property modifier for PANi. The thermal, thermomechanical, and morphological properties of the materials were also studied.

## EXPERIMENTAL

EPDM rubber (67, 28, and 5% ethylene, propylene, and ethylidene-norbornene, respectively) was purchased from DSM Americas (Brazilian plant) and used as received. HCl-doped PANi was prepared by an adaptation<sup>13</sup> of a previously reported work.<sup>14</sup> PANi-HCl was neutralized with NH<sub>4</sub>OH, producing the emeraldine base (EB). For reactive processing, EB was mixed with DBSA and EPDM in an internal mixer coupled to a Haake Rheocord 90, as described next.

### Mixture Preparation

PAni:DBSA stoichiometry was 1:2 in all mixtures prepared with 10, 20, and 30 wt % EPDM in the following sequence:

1. Loading of the mixer chamber simultaneously with PANi, DBSA, and EPDM at 150°C and 50 rpm.
2. Closure of the mixing chamber and recording of the torque as a function of time until a constant value was reached.
3. Discharge of the mixer chamber and lamination of the mixtures in an open roll mill at 60°C for the preparation of homogeneous films. The samples were laminated 3 and 36 times (cycle processes).

For comparison, we also doped EB by grinding it in a mortar with DBSA in a 1:2 ratio. This sample is called *nonprocessed* in the text.

### Characterization

Rheometric experiments were performed in an oscillating disc rheometer (Monsanto MDR 2000E) at 150°C for 30 min. Electrical conductivity was measured with an adaptation of the Coleman method with a Keithley 617 program-

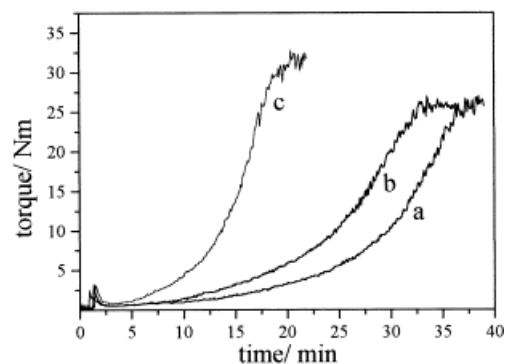


**Figure 1** Torque-mixing curves for PANi-DBSA with (a) 10, (b) 20, (c) 30 wt % EPDM.

mable electrometer and a four-probe sensor with gold contacts.<sup>15</sup> Conductivity versus stretching was carried out in an EMIC DL 2000. The samples were stretched in 1.0-mm steps, with the conductivity measured after 2 min with four flat, equally spaced alligator contacts at a distance of 10 mm with a Keithley 617 electrometer for measuring the current between the external contacts and for applying a potential of 1.0 V between the internal contact. Stress-strain properties were measured for eight test samples in an EMIC DL 2000 with a 50-N cell and a crosshead speed of 10 mm min<sup>-1</sup>. The samples were cut parallel or perpendicular to the lamination direction with dimensions of 100 × 15 × 0.15 mm. Differential scanning calorimetry (DSC) and thermogravimetric analysis (TGA) measurements were made with DuPont 910 and 951 instruments, respectively, under a N<sub>2</sub> atmosphere and at a heating rate of 10°C min<sup>-1</sup>. DSC curves were registered for a heating scan from 0 to 300°C. Thermomechanical analysis (TMA) measurements were carried out in a TA-2940 instrument in the compression mode and with a load of 0.05 N, from -100 to 300°C, under a N<sub>2</sub> atmosphere and at a heating rate of 10° min<sup>-1</sup>. Scanning electron microscopy (SEM) measurements were performed in a JEOL JSM-T300 scanning electron microscope with the backscattering electron technique and with samples coated with gold via sputtering.

## RESULTS AND DISCUSSION

### Rheological and Processing Characteristics

Melt-mixing torque-time curves for blends prepared with different compositions (at 150°C and 50 rpm) are shown in Figure 1. All the systems

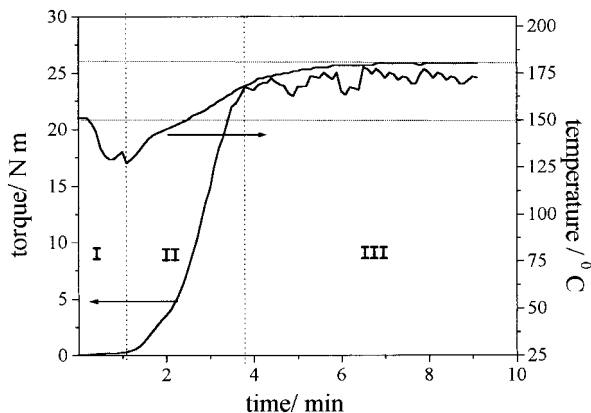


**Figure 2** Torque-temperature-mixing curves for PANi-DBSA.

show a torque increase. A rise in torque during mixing indicates a viscosity increase and is interpreted as the formation of crosslinks in a system with an increase in the molecular weight, as previously observed for other elastomeric blends.<sup>16,17</sup> The 70/30 PANi-DBSA/EPDM blend shows the highest torque increase rate, compared with the 80/20 and 90/10 blends. However, the opposite behavior would be expected if we consider that only PANi-DBSA undergoes crosslinking. Even so, some interactions occur between PANi-DBSA and EPDM simultaneously with the PANi doping process. The addition of EPDM dilutes the crosslinking reactions in the PANi chains and decreases the mixing time. Thus, EPDM could be considered the soft part of the blend, contributing to reducing the tension among the PANi chains. Pure EPDM does not show any rise in torque (the curve is not shown), whereas pure PANi-DBSA shows an increase up to 4 min (Fig. 2). The figure also shows that the temperature changes with the mixing time for the PANi-DBSA doping reaction during processing. Initially, the temperature drops below the temperature set with the addition of PANi EB and DBSA (stage I). After this, the torque begins to rise because of the protonation reaction (stage II); however, the torque rise is followed by a large increase in temperature. This may be assigned to the doping process and a crosslinking reaction, which is confirmed by the cure and DSC curves shown in Figures 3 and 4, respectively. Pereira da Silva and coworkers<sup>18,19</sup> studied the crosslinking mechanism of PANi as a function of temperature with Raman spectroscopy and observed the formation of a band at  $514\text{ cm}^{-1}$ , which they assigned to phenazine cyclic structures due to chain reticulations. The cure curve

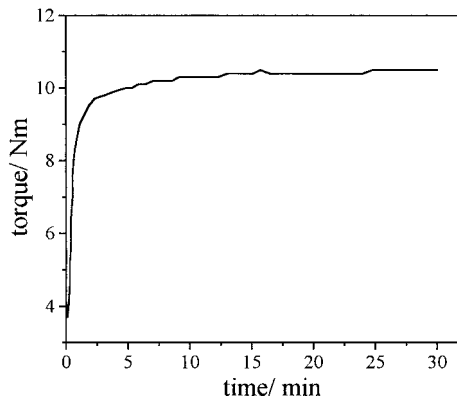


**Figure 3** Cure curve for PANi-DBSA.

(Fig. 3) was obtained in a Monsanto rheometer at  $150^{\circ}\text{C}$  for 30 min. This instrument consisted of a rotating disc and a cavity that contained the test sample. The test sample was cured in the cavity, whereas a disc embedded in the sample underwent an oscillatory rotation through a small arc. Resistance to the oscillation was measured and recorded as function of time. This equipment was used to characterize vulcanization reactions in rubber compounds and also supported the crosslinking reaction.<sup>20,21</sup> The observed increase in torque at a given time is directly related to the crosslinking density, particularly if the measurements are made at relatively low frequencies. This reaction can also be seen in the DSC curve (Fig. 4). The large peak around  $130^{\circ}\text{C}$  disappears after PANi-DBSA has been processed. This means that the exothermic reaction between acid and PANi could be due to incomplete PANi protonation accompanied by a reticulation reaction.<sup>11,12</sup> This is also confirmed by an increase in

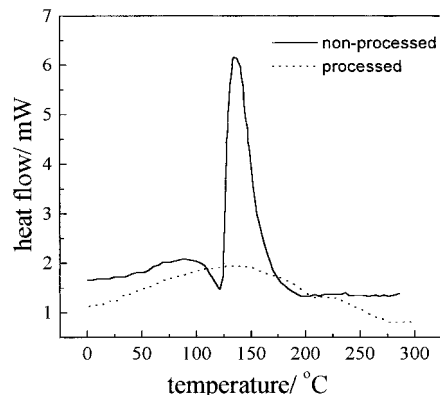


**Figure 4** DSC curves for PANi-DBSA (a) before and (b) after cure experiments.

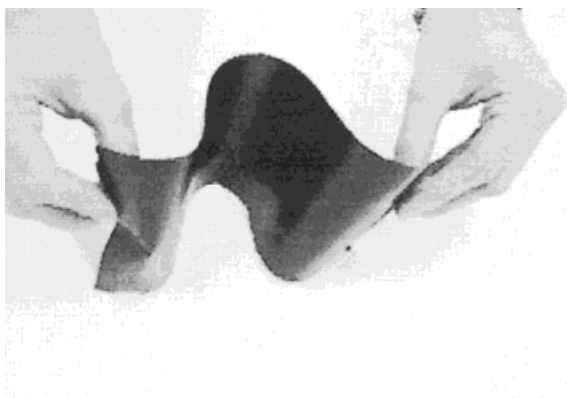


**Figure 5** Photograph of the laminated PANi-DBSA blend.

conductivity for the product. PANi conductivity was measured after the rheometric experiments and reached  $5.0 \text{ S cm}^{-1}$ . Below the phase transition, the conductivity is at a level typical of the ionic conductivity of liquid DBSA, whereas above the transition, conductivity levels can be increased by several orders of magnitude.

The mixture prepared in the internal mixer was transferred to an open roll mill and laminated; this produced flexible and self-supported films, as shown in Figure 5. Dumbbell test samples and strips were cut for stress-strain tests, thermal analysis, TMA, SEM, and conductivity measurements.

### Mechanical Properties and Morphological Characteristics

The stress-strain curve for an 80/20 PANi-DBSA/EPDM test sample cut parallel to the lamination direction is shown in Figure 6. The blend behaves like an elastomer because of the influence of the

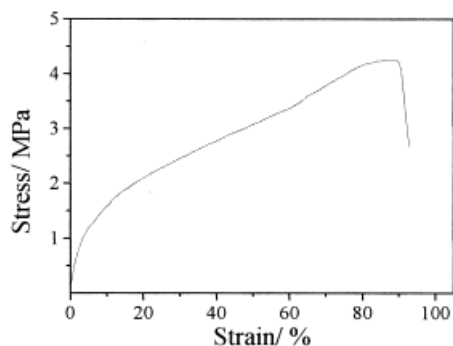


**Figure 6** Stress-strain curve for a parallel-cut PANi-DBSA/EPDM blend.

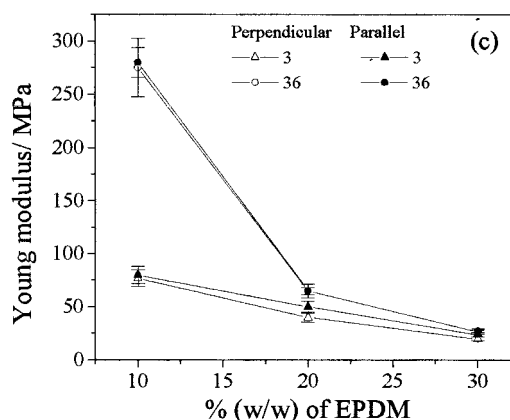
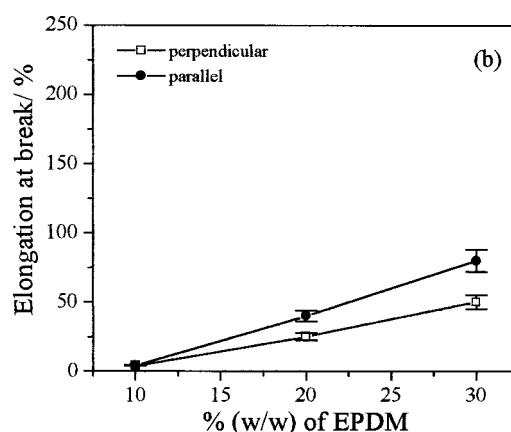
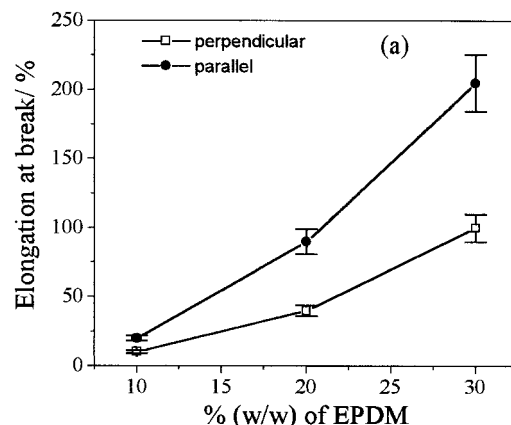
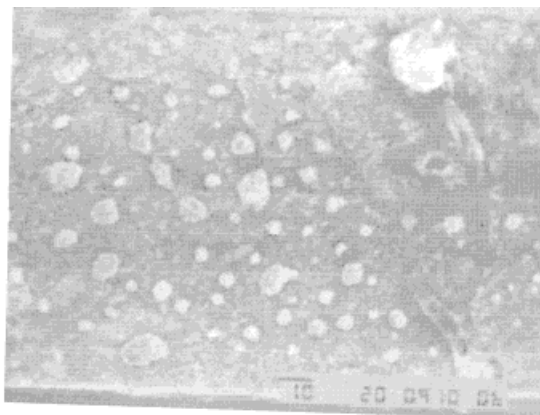
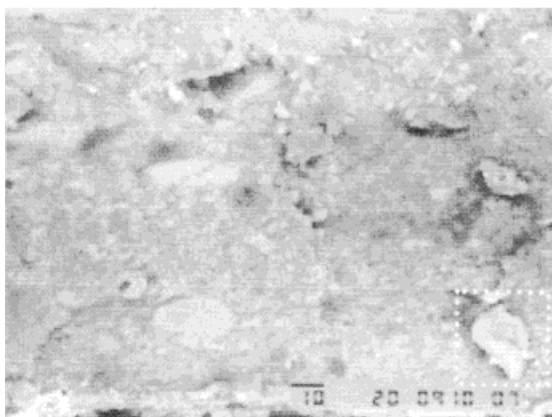


**Figure 7** (a,b) Elongation at break for PANi-DBSA/EPDM blends with 3 and 36 laminations, respectively, and (c) Young's modulus for PANi-DBSA/EPDM blends.

EPDM phase. Changes in the mechanical properties as a function of the EPDM content, number of lamination processes, and orientation of the sam-



(a)



(b)

**Figure 8** SEM images of (a) parallel-cut and (b) perpendicular-cut PANi-DBSA/EPDM films.

ple in relation to the lamination direction are shown in Figure 7(a–c). Parallel-cut samples exhibit a higher tension and elongation at break because the lamination process creates a chain alignment in the EPDM phases; however, intensive lamination (36 times) causes a decrease in the elongation at break assigned to an increase in the rigidity of the material. Surface morphology data elucidate the mechanical behavior; as presented in Figure 8, the dark regions correspond to the PANi-DBSA-rich phase, whereas the bright regions correspond to the EPDM-rich phase. The surfaces of films from 3 laminations [Fig. 8(a)] exhibit regular and well-distributed EPDM particles and good phase adhesion, whereas the surface of films laminated 36 times [Fig. 8(b)] show EPDM particles expelled from the film surface. This is assigned to phase segregation [see the boxed detail in Fig. 8(b)]. This effect explains the

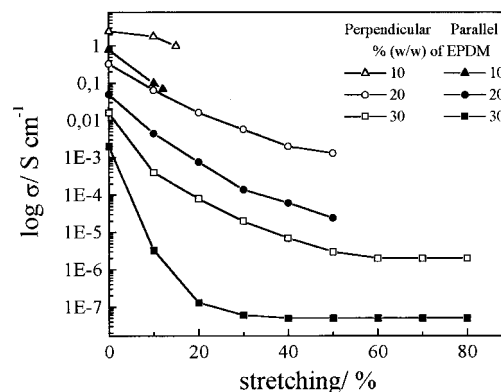


**Figure 9** Electrical conductivity versus stretching for blend films containing (a,b) 10, (c,d) 20, and (e,f) 30 wt % EPDM. Open symbols represent perpendicular-cut blends, and closed symbols represent parallel-cut blends.

decrease in the elongation at break of the films with intensive lamination.

The elongation at break shows a significant increase for mixtures with higher amounts of EPDM, and this is more accentuated for parallel-cut samples (Fig. 7). This behavior is repeated for mixtures prepared with either 3 or 36 laminations, despite the morphology changes. The variation of the modulus as a function of the rubber content is shown in Figure 7(c). The modulus decreases with increasing rubber content. For 10% EPDM, an abrupt modulus increase is observed for 36 laminations with respect to 3 laminations. This is due to phase segregation, as previously explained with morphological studies.

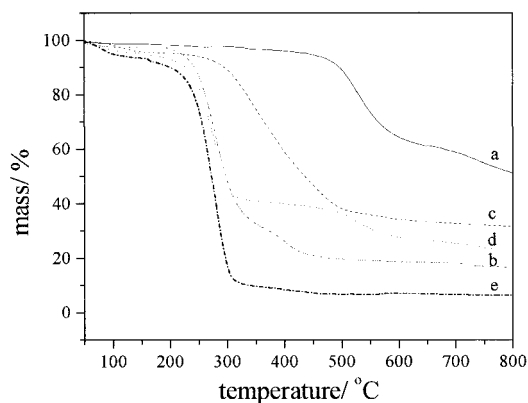


**Figure 10** TGA curves ( $N_2$  atmosphere,  $10^\circ C \text{ min}^{-1}$ ) for (a) dedoped PANi, (b) nonprocessed PANi-DBSA, (c) processed PANi-DBSA, (d) PANi and DBSA mixtures (calculated), and (e) DBSA.



## Electrical Conductivity

The conductivity values for films with 10, 20, and 30 wt % EPDM were  $10^{-1}$ ,  $10^{-2}$ , and  $10^{-3}$  S cm $^{-1}$ , respectively. The measurements of the conductivity for stressed samples indicated an overall decrease in conductivity with increased strain (Fig. 9). This can be assigned to a break in the conductive connections between the conductive phases of the blend, as previously observed by Mantovani et al.<sup>22</sup> in blends of PANi-CSA with a poly(styrene-ethylene-butylene-styrene) triblock copolymer. The effect is more pronounced for samples cut parallel to the lamination direction, as shown in Figure 9. Other authors have observed that the conductivity increases with the uniaxial orientation of PANi films and fibers.<sup>23</sup> The inverse behavior observed in our samples can be assigned to the preparation method used; other authors have used solution casting to prepare films, and stretching induces chain orientation. In our work, the EPDM rubber only agglomerates the PANi particles, not allowing chain alignment in the particles.

## Thermal Properties

We studied the thermal behavior of the mixtures and pure components (EPDM, DBSA, and PANi). Also, we performed a comparison of the thermodegradation of processed and nonprocessed PANi-DBSA to elucidate the processing effect. Here, nonprocessed PANi-DBSA is a physical mixture prepared by the grinding of EB and DBSA in a mortar in a 1:2 ratio, producing doped PANi.<sup>24</sup>

As shown in Figure 10(b), the thermodecomposition process of nonprocessed PANi-DBSA occurs in three stages of mass loss. The first stage, about 5% and below 150°C, is presumably due to humidity loss; the second, 62% of the total mass and between 200 and 340°C, is due to acid degradation. The amount of acid present in the mixture is 64%, which means that almost all the acid is degraded in this stage.<sup>25</sup> After this stage, the remaining PANi is dedoped, and so the last mass loss corresponds to the degradation of PANi EB [Fig. 10(a)]. For PANi-DBSA doped by reactive processing [Fig. 10(c)], two thermodecomposition stages are observed and assigned to humidity loss and PANi-DBSA degradation. Increases in stability (shift of the temperature onset) and in the amounts of residues are observed. The residues might be due to the reaction between the components produced by crosslinked stable structures.

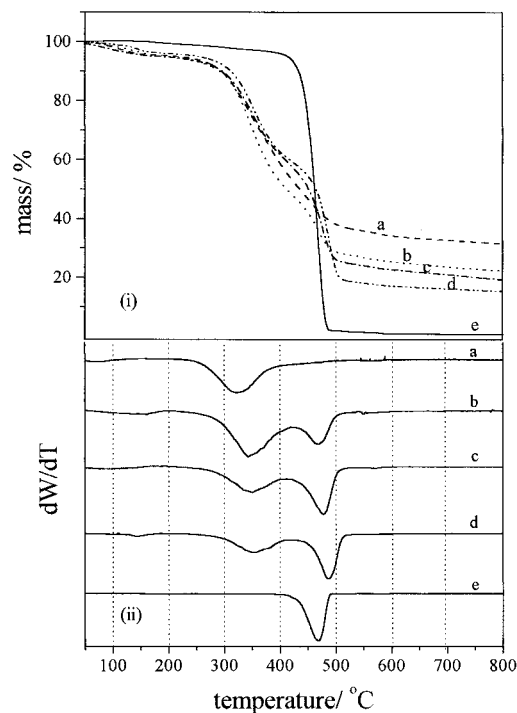


**Figure 11** (i) TGA and (ii) first derivative curves (N<sub>2</sub> atmosphere, 10°C min $^{-1}$ ) for (a) processed PANi-DBSA; (b-d) PANi-DBSA blends with 10, 20, and 30 wt % EPDM, respectively; and (e) pure EPDM.

In agreement with Waldman and De Paoli,<sup>26</sup> interaction effects between the components of a polymer mixture can be visualized by a comparison of the experimental curves of the pure polymers, the curve for the mixture, and the curves simulated by the averaging of the curves of the pure components. These interactions may retard or accelerate the degradation processes. If the mixture components do not interact, the averaged curve superimposes the experimental curve. The curve simulated by the averaging of DBSA and dedoped PANi curves [Fig. 10(d)] shows that processing provides not only physical but also chemical interactions among the components, here called doping. The stability increases and the curve slope is different for both curves, indicating that the degradation rate is higher for processed PANi-DBSA [Fig. 10(c)] than for the nonprocessed sample [Fig. 10(b)].

TGA curves for PANi-DBSA/EPDM blends show three degradation stages, curves b, c, and d in Figure 11(i,ii). By comparing these curves with the curves for processed PANi-DBSA (curve a) and pure EPDM (curve e), we can assign the first mass loss step of the blends, from 25 to 180°C, to humidity loss. The second stage, from 250 to

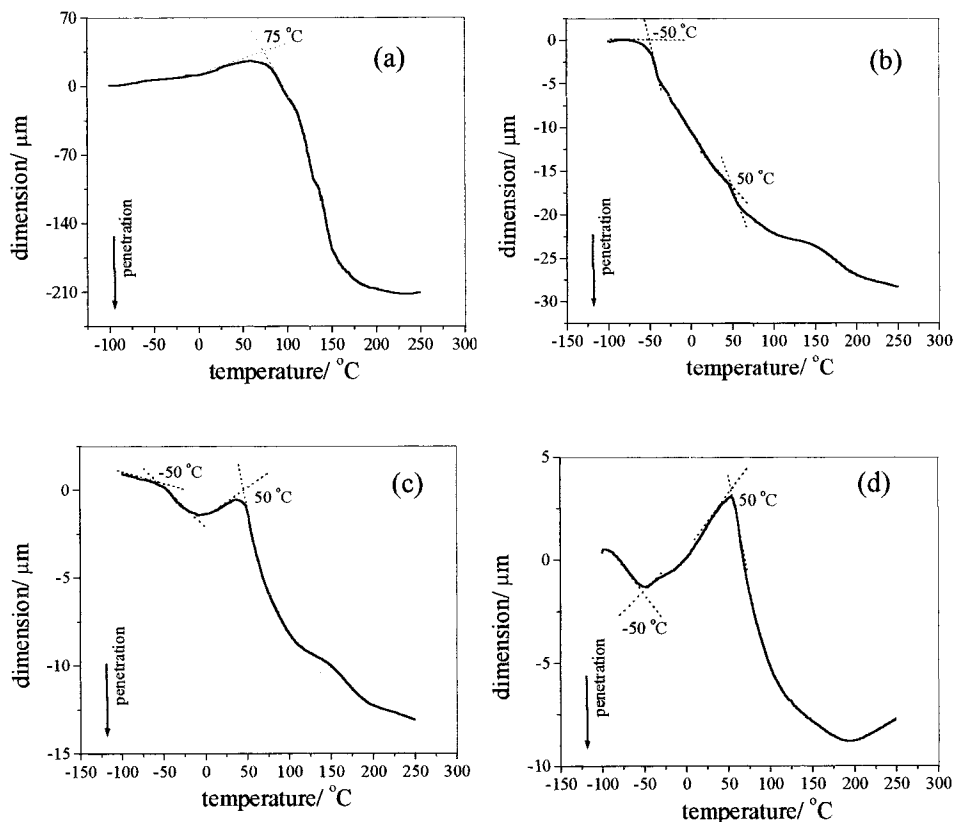


**Figure 12** TMA curves ( $N_2$  atmosphere,  $10^\circ C \text{ min}^{-1}$ ) for (a) processed PANi-DBSA; (b–d) PANi-DBSA blends with 10, 20, and 30 wt % EPDM, respectively; and (e) pure EPDM.

$400^\circ C$ , is assigned to PANi-DBSA degradation, and the last one, above about  $450^\circ C$ , is assigned to EPDM degradation. EPDM degradation in the blend is retarded for blends with 20 and 30 wt % EPDM. This behavior is better shown in the differential curves in Figure 11(ii). This indicates some interactions among the blend components. Dedoping of PANi-DBSA (or DBSA degradation) is not observed; this indicates that EPDM does not preclude the protonation of PANi, as shown by the torque curves.

By analyzing the final residues in the TGA curves of Figure 11(i), we observe for processed pure PANi-DBSA 40% residual mass, whereas the calculated value would be 33%. The increase in the residual mass is assigned to crosslinking, as discussed previously. For the blend containing 10 wt % EPDM, the residual mass observed is 30%, agreeing with the calculated value. However, for blends containing 20 and 30% EPDM, the mass residues observed, 25 and 18%, are lower than those calculated, 27 and 33%, respectively. This provides evidence of the chemical in-

teraction of EPDM decomposition products and PANi that reduces crosslinking.

### Thermomechanical Properties

TMA measures the dimensional changes or penetration into a material, with time, temperature, or load (or stress) as the independent variables. In this work, the penetration mode was used. The softening associated with the large-scale decrease in the modulus at the glass-transition temperature ( $T_g$ ) was measured in this mode.  $T_g$  is observed as an inflection in the curve. Figure 12(a–d) presents the TMA measurements for PANi-DBSA and PANi-DBSA/EPDM blends. Figure 12(a) shows the changes that occur during the heating of PANi-DBSA. At about  $75^\circ C$ , the sample begins to soften (height decreases), and this softening temperature has been correlated with  $T_g$ . Ikkala et al.<sup>27</sup> verified that the  $T_g$  of PANi-DBSA is completely dependent on the DBSA concentration. For example, the  $T_g$  value decreases as the acid concentration increases for  $x = 0.7$  and

1.5, where  $T_g$  is 130 and 65°C, respectively. Wei et al.<sup>28</sup> described the  $T_g$  of NMP-solution-cast films of PANi EB. The  $T_g$  of the EB films was strongly dependent on the content of the residual NMP solvent. For films containing about 16–0% residual NMP, the  $T_g$  was determined to be between 105 and 220°C.

TMA curves for PANi–DBSA/EPDM blends show some differences [Fig. 12(b–d)]. Two changes in the dimensions observed for the PANi–DBSA/EPDM blends are assigned to the EPDM and PANi–DBSA  $T_g$ 's (–50 and 50°C, respectively). For blends with 10 wt % EPDM, there is no distinction between the  $T_g$ 's [Fig. 12(b)]. This can be related to the partial miscibility of EPDM and PANi–DBSA, whereas DBSA acts as a compatibilizer. For blends with 20 wt % EPDM, the  $T_g$  separation is more pronounced [Fig. 12(c)]. This can be due to the increase in the EPDM content, which contributes to phase separation. This can be better shown for blends with 30 wt % EPDM [Fig. 12(d)]. After the  $T_g$  of EPDM (–50°C), the material becomes rigid, as indicated in the curve by an expansion. This behavior can be explained by the crosslinking of the EPDM phase. This leads to a more pronounced separation of the  $T_g$  values of EPDM and PANi–DBSA. The third dimensional change (ca. 150°C) can be assigned to crosslinking.

## CONCLUSION

We have demonstrated that the addition of EPDM to PANi–DBSA produces materials with elastomeric characteristics and good conductivity performance. The processing method used in this work provides a good way for producing conductive films on an industrial scale.

The assistance of P. S. de Freitas in preparing the polyaniline is acknowledged.

## REFERENCES

- Cao, Y.; Smith, P.; Heeger, A. J. *Synth Met* 1992, 48, 91.
- Cao, Y.; Smith, P. *Synth Met* 1995, 69, 191.
- Cao, Y.; Smith, P.; Heeger, A. J. *Synth Met* 1993, 57, 3541.
- Cao, Y.; Smith, P.; Heeger, A. J. *Synth Met* 1993, 53, 293.
- Prón, A.; Laska, J.; Osterholm, J. E. *Polymer* 1993, 34, 4235.
- Prón, A.; Osterholm, J. E.; Smith, P.; Heeger, A. J.; Laska, J.; Zagorska, M. *Synth Met* 1993, 55–57, 3514.
- Laska, J.; Prón, A.; Lefrant, S. *J Polym Sci Part A: Polym Chem* 1995, 33, 1437.
- Abell, L.; Pomfret, S.; Adams, P. N.; Middleton, A. C.; Monkaman, A. P. *Synth Met* 1997, 84, 803.
- van der Wal, A.; Nijhof, R.; Gaymans, R. J. *Polymer* 1999, 40, 6031.
- Bucknall, C. B. *Adv Polym Sci* 1978, 27, 121.
- Levon, K.; Ho, K.-H.; Zheng, W.-Z.; Laakso, J.; Kärnä, T.; Taka, T.; Österholm, J.-E. *Polymer* 1995, 36, 2733.
- Ikkala, O. T.; Laakso, J.; Vakiparta, K.; Virtanen, E.; Ruohonen, H.; Jarvinen, H.; Taka, T.; Passinemi, P.; Osterholm, J.-E. *Synth Met* 1995, 69, 97.
- Freitas, P. S. Ph.D. Thesis, UNICAMP, Campinas, Brasil, 2000.
- Gazotti, W. A.; De Paoli, M.-A. *Synth Met* 1996, 80, 263.
- Coleman, L. B. *Rev Sci Instrum* 1975, 46, 1125.
- Manoj, N. R.; De, P. P. *Polymer* 1998, 39, 733.
- Zhu, S.; Chan, C.-M. *Polymer* 1998, 26, 7023.
- Pereira da Silva, J. E.; Faria, D. L. A.; Córdoba de Torresi, S. I.; Temperini, M. L. A. *Macromolecules* 2000, 33, 3077.
- Pereira da Silva, J. E.; Córdoba de Torresi, S. I.; Temperini, M. L. A. *J Braz Chem Soc* 2000, 11, 91.
- Coran, A. Y. *CHEMTECH* 1983, 2, 106.
- Coran, A. Y. *Rubber Chem Technol* 1964, 37, 679.
- Mantovani, G. L.; MacDiarmid, A. G.; Mattoso, L. H. C. *Synth Met* 1997, 84, 73.
- Adams, P. N.; Laughlin, P. J.; Monkman, A. P. *Solid State Commun* 1994, 91, 875.
- Faez, R.; De Pooli, M.-A. *Eur Polym J* 2001, 37, 1139.
- Zilberman, M.; Titelman, G. I.; Siegmann, A.; Haba, Y.; Narkis, M.; Alperstein, D. *J Appl Polym Sci* 1997, 66, 243.
- Waldman, W. R.; De Paoli, M.-A. *Polym Degrad Stab* 1997, 60, 301.
- Ikkala, O. T.; Lindholm, T. M.; Ruohonen, H.; Seläntaus, M.; Väkiparta, K. *Synth Met* 1995, 69, 135.
- Wei, Y.; Jang, G. W.; Hsueh, K. F.; Scherr, E. M.; MacDiarmid, A. G.; Epstein, A. J. *Polymer* 1992, 33, 314.